Functional Coordination Polymers

DOI: 10.1002/anie.201008277

Phosphorescent Nanoscale Coordination Polymers as Contrast Agents for Optical Imaging**

*Demin Liu, Rachel C. Huxford, and Wenbin Lin**

Optical imaging, which uses neither ionizing radiation (as in X-ray computed tomography) nor radioactive materials (as in positron emission tomography or single-photon emission computed tomography),[1] has emerged as a powerful imaging modality during the last two decades.[2] Optical imaging has been widely employed for oncological and other applications owing to its ability to noninvasively differentiate between diseased (e.g., tumor) and healthy tissues on the basis of differential dye accumulations.[3] The need for relatively high (up to micromolar) concentrations of dyes in optical imaging, however, limits its application in many areas, such as detecting low concentrations of biological targets. For example, many biomarkers are overexpressed in the nanomolar concentration range in diseased tissues[4] and cannot be readily visualized by optical imaging. Dye-loaded nanoparticles represent a logical solution to lowering the detection limit, owing to their ability to carry a large payload of dye molecules as well as to target certain cell types by conjugation to affinity molecules. Luminescent quantum dots have indeed been extensively explored as bright and stable contrast agents for optical imaging.[5] The nondegradable nature and the use of toxic elements in many quantum dot formulations, however, limit their applications in many areas. Most fluorescent dye molecules, on the other hand, have small Stokes shifts and tend to have a significant overlap between absorption and fluorescence emission spectra. As a result, these fluorescent dyes can suffer from severe self-quenching if they are brought into close proximity with each other, as in nanoparticles with high dye loadings.

Luminescence originating from nonsinglet states of metal complexes tends to have long lifetimes and large Stokes shifts. We hypothesize that highly luminescent nanoparticles can be constructed from such dye molecules, as they will not undergo self-quenching owing to large Stokes shifts.[6,7] Herein we report the synthesis, characterization, and preliminary applications of biodegradable, phosphorescent nanoscale coordination polymers in in vitro optical imaging.

[*] D. Liu, R. C. Huxford, Prof. W. Lin
Department of Chemistry, CB#3290, University of North Carolina
Chapel Hill, NC 27599 (USA)
Fax: (+1) 919-962-2388
E-mail: wlin@unc.edu
Homepage: http://www.chem.unc.edu/people/faculty/linw/wlindex.html

[**] We thank the NIH-NCI (U01-CA151455) for financial support and Mr. Caleb A. Kent and Cheng Wang for experimental help.

Supporting information for this article is available on the WWW under http://dx.doi.org/10.1002/anie.201008277.

Coordination polymers, also called metal–organic frameworks, are an interesting class of hybrid materials constructed from metal-ion or metal-cluster connecting points and molecular bridging ligands.[8] Molecular tunability of such hybrid materials has allowed the design of coordination polymers for a wide range of applications, such as gas storage,[9] nonlinear optics,[10] chemical sensing,[11] and catalysis.[12] We and others recently demonstrated the ability to scale down these materials to the nanoregime to afford nanoscale coordination polymers (NCPs) for potential biological and biomedical applications.[13] For example, NCPs have been shown to be applicable to biosensing,[14] magnetic resonance imaging,[15] computed tomography,[16] and drug delivery.[17] In this work, we synthesized phosphorescent NCPs using the $[Ru\{5,5'\text{-}(CO_2)_2\text{-bpy}\}(bpy)_2]$ bridging ligand (bpy is 2,2′-bipyridine) and Zn^{2+} or Zr^{4+} connecting points. The zinc and zirconium NCPs have dye loadings of 78.7% and 57.4%, respectively. The zirconium NCP was further stabilized with a silica coating and functionalized with poly(ethylene glycol) (PEG) and a targeting molecule for in vitro optical imaging of cancer cells.

The phosphorescent ruthenium complex $[Ru\{5,5'\text{-}(CO_2H)_2\text{-bpy}\}(bpy)_2](PF_6)_2$ ($[L\text{-}H_2](PF_6)_2$) was synthesized by treating $5,5'\text{-}(CO_2Et)_2$-bpy with $[Ru(bpy)_2Cl_2]$ and subsequent acid-catalyzed hydrolysis and anion exchange.[18] The bulk zinc coordination polymer with the formula $[Zn_2L\text{-}(C_2O_4)_2]\cdot 2\,dmf\cdot 3\,H_2O$ (**1**) was synthesized by allowing $Zn(NO_3)_2$ and $[L\text{-}H_2](PF_6)_2$ to react in a dimethylformamide (dmf) and H_2O mixture in a screw-capped vial at 90 °C for two days. Compound **1** crystallizes in the triclinic space group $P\bar{1}$ with one L ligand, two Zn atoms, and two oxalate molecules in the asymmetric unit.[18] The Zn center is coordinated by five oxygen atoms, one from the carboxylate group of the L ligand and the other four from the oxalate molecules, to form a 2D bilayer structure (Figure 1a,b). Packed along the *b* axis, the 2D layers have a distance of 4.8 Å between bpy planes of adjacent layers. The shortest distance between the two Ru centers within the bilayer is 9.4 Å. The phase purity of **1** is supported by a good match of the powder X-ray diffraction (PXRD) pattern of the pristine sample and the simulated pattern from the single-crystal structure. The complete formulation of **1** was established by single-crystal X-ray diffraction studies, NMR spectroscopy, and thermogravimetric analysis (TGA) results (see the Supporting Information).

Dark orange, crystalline nanoparticles of **1** (NCP-**1**) were synthesized in 54.3% yield by microwave heating of a solution of $[L\text{-}H_2](PF_6)_2$, oxalic acid, and $Zn(NO_3)_2$ in dmf/H_2O at 100 °C for 5 min. SEM images show that NCP-**1** forms blocklike particles that have dimensions of approximately $100 \times 100 \times 50$ nm (Figure 1c). PXRD studies indicate that the

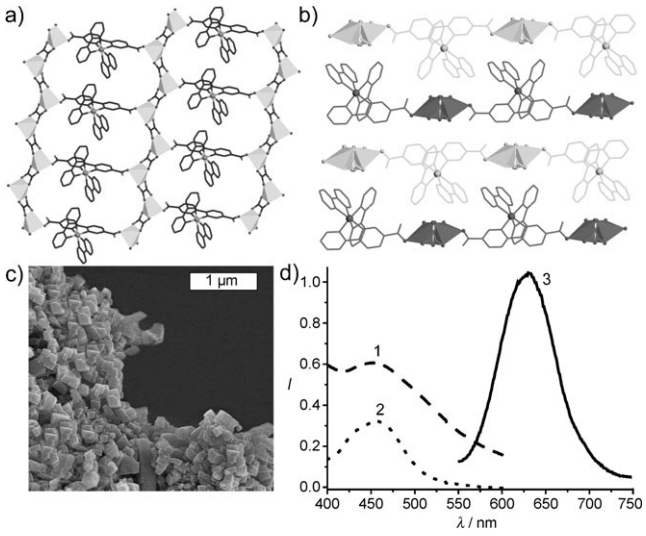

Figure 1. a) A top view of the 2D layer of **1** down the *b* axis. b) A side view along the *a* axis showing the packing of the 2D layers in **1**. c) SEM image of NCP-**1**. d) Absorption (1) and emission (3) spectra of NCP-**1** in ethanol. The absorption spectrum of dissolved NCP-**1** (2) was also taken to eliminate the scattering effects.

NCP-**1** particles are crystalline and share the same phase as bulk crystals of **1**. The UV/Vis spectrum of a dispersion of NCP-**1** in ethanol shows a broad metal-to-ligand charge transfer (MLCT) absorption band between 400 and 550 nm. NCP-**1** has a luminescence quantum yield of 2.1%; the normalized emission spectrum ($\lambda_{max} \approx 635$ nm) is shown in Figure 1d. The time-resolved emission transient for NCP-**1** monitored at 630 nm was fit to biexponential decay kinetics,[19] giving an average lifetime of 215 ns.

As the NCP-**1** particles rapidly dissolve in water and biologically relevant media, we attempted to stabilize them by encapsulation with a silica coating. We previously used the strategy of coating NCPs with a thin layer of silica to tune the kinetics of cargo release from NCPs.[14,17] Silica coatings can also enhance biocompatibility and water dispersibility.[17,20] Unfortunately, NCP-**1** was not stable under the coating conditions, as the L dye molecules leached from the particles, and the recovered particles were nearly colorless. The decomposition of NCP-**1** under the coating conditions was corroborated by SEM and energy-dispersive X-ray spectroscopy (EDS) data (see the Supporting Information).

We speculate that more stable NCPs can be synthesized if Zr^{4+} ions are used in place of Zn^{2+} to connect carboxylate groups of the L ligands, as the UiO (Universitetet i Oslo) materials composed of Zr^{4+} ions and dicarboxylate bridging ligands were shown to be among the most stable coordination polymers synthesized.[21] Microwave heating of an acidic solution of $[L\text{-}H_2](PF_6)_2$ and $ZrCl_4$ in dmf at 100 °C for 10 min led to dark orange particles of NCP-**2** after centrifugation and washing with methanol and ethanol (Scheme 1). As shown in Figure 2a, SEM and TEM images showed that particles of **2** adopt a spherical morphology with an average diameter of 85 nm. NCP-**2** is amorphous, as judged by the lack of peaks in the PXRD pattern. Dynamic light scattering (DLS) measurements afforded a hydrodynamic diameter of (104 ± 4) nm for particles of **2** in ethanol (Figure 2d and Table 1). The absorption and emission spectra are shown in Figure 2e; to eliminate scattering effects, the absorption spectrum was also taken after digesting NCP-**2** with sodium hydroxide (6 M, aq.). NCP-**2** has a luminescent quantum yield of 0.8% and an average luminescence lifetime of 107 ns (at 630 nm). Dye loadings of 57.4% and 55.0% were calculated from TGA and inductively coupled plasma mass spectrometry (ICP-MS) results, respectively (Table 1).

The as-synthesized particles of **2** are very stable in water but rapidly decompose in 8 mM phosphate-buffered saline (PBS) at 37 °C with a half-life ($t_{1/2}$) of about 0.5 h, presumably owing to the strong driving force provided by the formation of zirconium phosphates. To slow down the release of L dye molecules from **2** in biologically relevant media, we attempted to coat the particles with a thin shell of silica. To our delight, NCP-**2** is stable under the coating conditions, and the presence, after the coating procedure, of a thin layer of silica on particles of **2** was confirmed by TGA, EDS (see the Supporting Information), DLS, and release profile data (Figure 2d,f, and Table 1). TGA gave a 12.5% reduction in the total weight loss for the particles of SiO_2@**2** compared to NCP-**2**. The DLS Z-average diameter for SiO_2@**2** is approx-

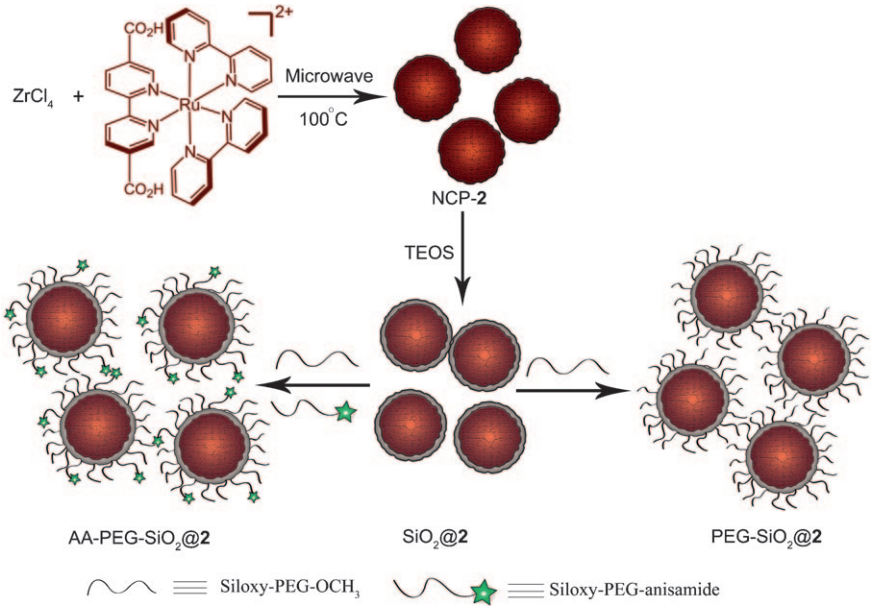

Scheme 1. Synthesis of NCP-**2**, coating of NCP-**2** with a thin shell of silica, and further functionalization of SiO_2@**2** with PEG and PEG-anisamide. TEOS = tetraethylorthosilicate.

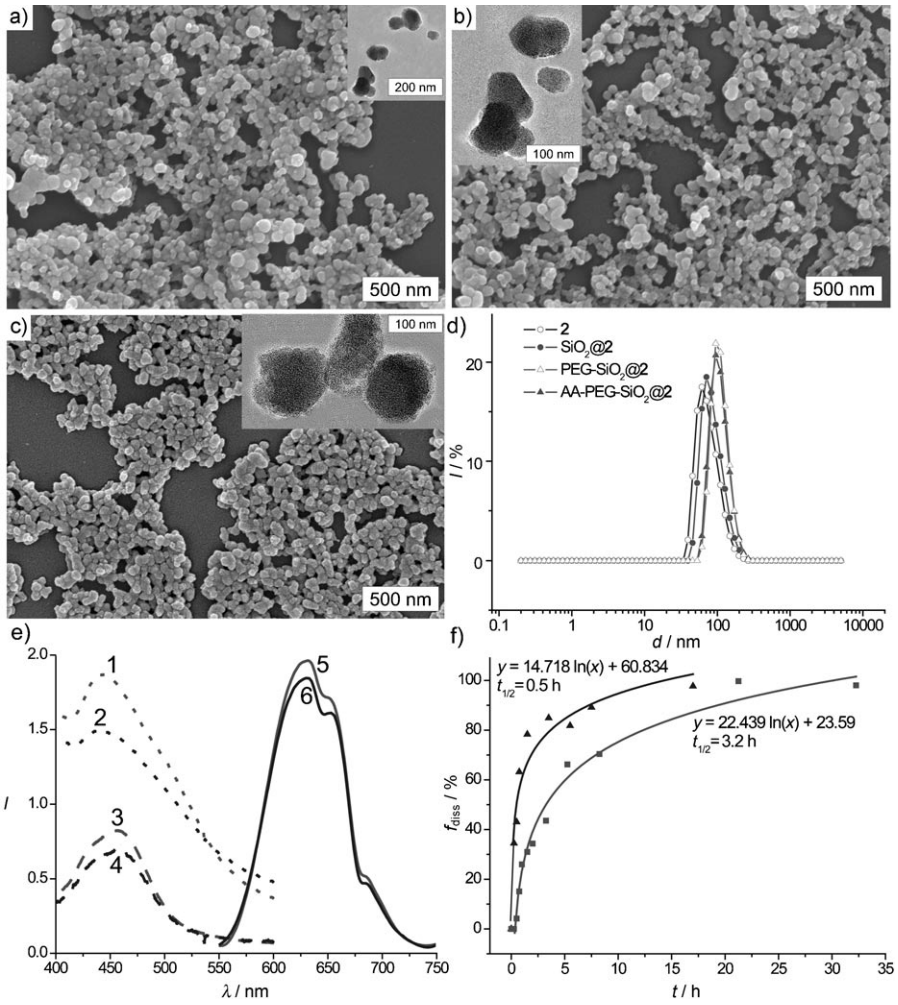

Figure 2. a–c) SEM and TEM (inset) images of NCP-**2** (a), SiO_2@**2** (b), and AA-PEG-SiO_2@**2** (c). d) Number-averaged size distribution (d = diameter) for NCP-**2** (○), SiO_2@**2** (●), PEG-SiO_2@**2** (△), and AA-PEG-SiO_2@**2** (▲) in ethanol. e) Absorption (1–4) and normalized emission spectra (5, 6) for NCP-**2** (1), AA-PEG-SiO_2@**2** (2), NCP-**2** after digestion (3), AA-PEG-SiO_2@**2** after digestion (4), NCP-**2** (5), and AA-PEG-SiO_2@**2** (6). f) Release profiles (f_{diss} = fraction of dissolved material) of NCP-**2** (▲) and SiO_2@**2** (■) in 8 mM PBS at 37 °C.

Table 1: Summary of characterization data for NCP-**2** and related particles.

Particle	d[a] [nm]	PDI[b]	Zeta potential [mV]	Dye loading [%]	
				TGA	ICP-MS
NCP-**2**	104 ± 4	0.205	−11.9 ± 3.2	57.4	55.0
SiO_2@**2**	107 ± 4	0.135	−34.4 ± 4.1	34.4	28.5
PEG-SiO_2@**2**	122 ± 10	0.103	−9.23 ± 1.9	32.9	27.6
AA-PEG-SiO_2@**2**	124 ± 7	0.062	−8.17 ± 2.8	32.7	27.0

[a] Z-average diameter. [b] Polydispersity index.

imately 3 nm larger than that of **2**. SiO_2@**2** has a zeta potential of (−34.4 ± 4.1) mV, which is about 22 mV more negative than that of **2** ((−11.9 ± 3.2) mV). The release profile of SiO_2@**2** in 8 mM PBS at 37 °C gave a $t_{1/2}$ of 3.2 h (Figure 2 f). The half-life of SiO_2@**2** particles is long enough for preliminary optical imaging experiments with cancer cells.

Silica coatings also provide surface silanol groups for further functionalization with other molecules containing siloxy groups. Surface modification with PEG, a relatively inert hydrophilic polymer, can prevent particle aggregation and increase the dispersibility of nanoparticles. The end of the PEG chain can be further modified to contain affinity molecules that target certain biomarkers. For example, sigma-1 and sigma-2 receptors are overexpressed in a wide variety of human tumor cells,[22] which makes it possible to use sigma-receptor binding ligands, such as anisamide, for tumor targeting.[23] Therefore, SiO_2@**2** was coated with CH_3O-PEG_{2000}-$Si(OEt)_3$ or with CH_3O-PEG_{2000}-$Si(OEt)_3$ and anisamide-PEG_{2000}-$Si(OEt)_3$ in a 9:1 molar ratio to afford PEGylated and targeted particles, PEG-SiO_2@**2** and AA-PEG-SiO_2@**2**, respectively. The PEG-SiO_2@**2** and AA-PEG-SiO_2@**2** particles appeared less aggregated (Figure 2 c), and a rougher edge around the particles was observed by TEM (inset in Figure 2 c). TGA gave a 1.5% increase in the total weight loss, and DLS measurements gave diameters of (122 ± 10) and (124 ± 7) nm for PEG-SiO_2@**2** and AA-PEG-SiO_2@**2** and zeta potentials of (−9.23 ± 1.9) and (−8.17 ± 2.8) mV, respectively. These results confirm the presence of the polymer coating.

To evaluate the potential use of NCP-**2** as a contrast agent for optical imaging, we conducted in vitro viability assays on H460 human non-small-cell lung cancer cells. Treatment of H460 cells with PEG-SiO_2@**2** and AA-PEG-SiO_2@**2** did not lead to any appreciable cell death after 24 h of incubation (Figure 3 d). To test their in vitro imaging contrast efficiency and targeting capacity, laser scanning confocal fluorescence microscopy studies were performed. As shown in Figure 3 a–c, significant MLCT luminescent signal was observed in the confocal z section images for H460 cells incubated with AA-PEG-SiO_2@**2**. In comparison, less luminescence was observed for H460 cells incubated with the non-targeted PEG-SiO_2@**2**. This result is further supported by an uptake study. After 24 h of incubation with H460 cells, the cells were isolated by centrifugation and washed with PBS. Cell pellets were digested in concentrated HNO_3 and Ru content was analyzed by ICP-MS. Enhanced uptake was observed for AA-PEG-SiO_2@**2** (Figure 3 e).

In conclusion, we have successfully synthesized phosphorescent nanoscale coordination polymers with extremely high dye loadings. The zirconium-based NCPs were stabilized with thin shells of amorphous silica to prevent rapid release from

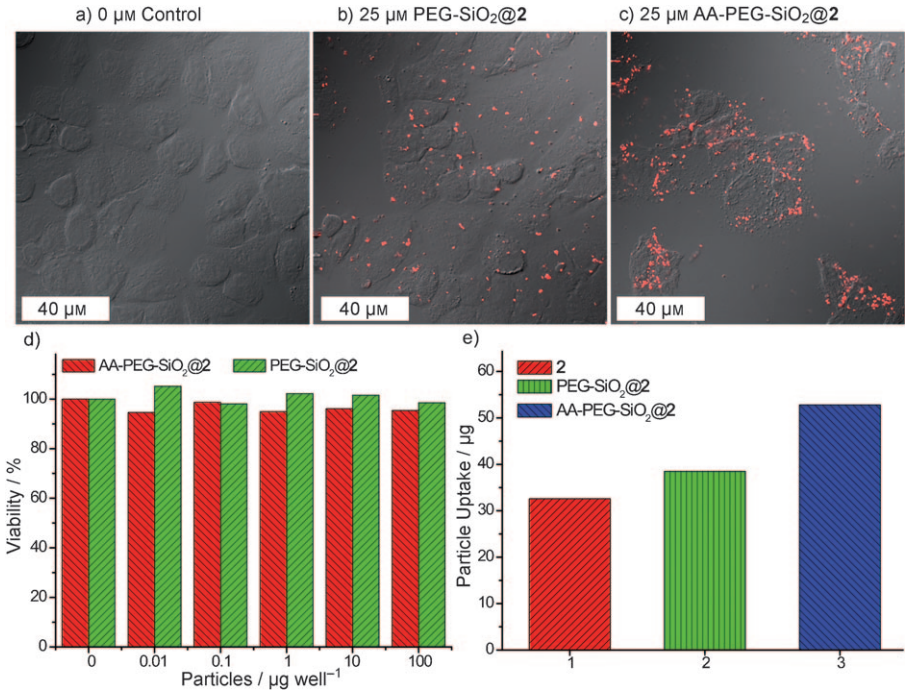

Figure 3. a–c) Confocal microscopy images of H460 cells that have been incubated without any particles (a), with PEG-SiO_2@**2** (b), and with AA-PEG-SiO_2@**2** (c). d) In vitro viability assay for H460 cells incubated with various amounts of PEG-SiO_2@**2** and AA-PEG-SiO_2@**2**. e) Particle uptake studies in H460 cells.

the nanoparticles, and the biocompatibility and targeting efficiency of the NCP/silica core–shell nanostructures was further improved by coating with PEG and PEG–anisamide. The anisamide-targeted particles are efficient optical imaging contrast agents and exhibit cancer specificity, as demonstrated by uptake studies and confocal microscopy of H460 cells in vitro. This work highlights the potential of nanoscale coordination polymers as a novel platform for the design of luminescent hybrid nanoparticles with extremely high dye loadings for optical imaging.

Experimental Section

NCP-**1**: $([L\text{-}H_2](PF_6)_2$ (5 mg, 0.005 mmol) and $Zn(NO_3)_2{\cdot}6H_2O$ (10 mg, 0.035 mmol) were dissolved in a mixture of dmf/H_2O (2.5 mL/0.1 mL). After the addition of HCl (15 μL, 3 M, aq.) and oxalic acid (5 μL, 0.75 M, dmf), the resulting solution was sealed in a microwave vial and placed in the microwave oven at 300 W. After 5 min of heating at 100 °C without stirring, the crystalline NCP-**1** particles were isolated by centrifugation at 13000 rpm for 15 min. The particles were washed once with dmf and three times with EtOH to afford approximately 4 mg of NCP-**1** (54.3 % yield).

Silica coating: NCP-**2** particles (4 mg) were dispersed in NH_3 (10 mL, 0.2 M, aq.) in ethanol (10 mL). TEOS (16 μL) was added to the dispersion, which was stirred magnetically, at room temperature. After 5 h, nanoparticles were isolated by centrifugation at 13000 rpm for 15 min, washed with dmf and ethanol, and re-dispersed in ethanol by sonication.

PEGylation and targeting: The SiO_2@**2** particles were diluted with ethanol to a final concentration of 3 mg mL^{-1}. Siloxy-PEG_{2K}-anisamide and siloxy-PEG_{2K}-OCH_3 were added to this dispersion in a molar ratio of 1 to 9 (1 mg PEG per 1 mL EtOH), and the resulting mixture was magnetically stirred under basic conditions (NH_3, 0.3 M aq.) at room temperature for 24 h. The anisamide-targeted particles were isolated by centrifugation, washed with ethanol, and redispersed in ethanol by sonication.

Received: December 30, 2010
Published online: March 17, 2011

Keywords: imaging agents · nanoparticles · optical imaging · organic–inorganic hybrid composites

[1] J. Fujimoto, D. Farkas, *Biomedical Optical Imaging*, First ed., Oxford University Press, New York, **2009**.
[2] a) V. Ntziachristos, J. Ripoll, L. V. Wang, R. Weissleder, *Nat. Biotechnol.* **2005**, *23*, 313; b) H. Kobayashi, M. Ogawa, R. Alford, P. L. Choyke, Y. Urano, *Chem. Rev.* **2010**, *110*, 2620; c) C. Kim, C. Favazza, L. V. Wang, *Chem. Rev.* **2010**, *110*, 2756.
[3] a) M. Nahrendorf, E. Keliher, B. Marinelli, P. Waterman, P. F. Feruglio, L. Fexon, M. Pivovarov, F. K. Swirski, M. J. Pittet, C. Vinegoni, R. Weissleder, *Proc. Natl. Acad. Sci. USA* **2010**, *107*, 7910; b) C. M. Cobley, J. Chen, E. C. Cho, L. V. Wang, Y. Xia, *Chem. Soc. Rev.* **2011**, *40*, 44; c) T. Nam, S. Park, S. Y. Lee, K. Park, K. Choi, I. C. Song, M. H. Han, J. J. Leary, S. A. Yuk, I. C. Kwon, K. Kim, S. Y. Jeong, *Bioconjugate Chem.* **2010**, *21*, 578.
[4] a) K. Kikuchi, *Chem. Soc. Rev.* **2010**, *39*, 2048; b) M. M. C. Cheng, G. Cuda, Y. L. Bunimovich, M. Gaspari, J. R. Heath, H. D. Hill, C. A. Mirkin, A. J. Nijdam, R. Terracciano, T. Thundat, M. Ferrari, *Curr. Opin. Chem. Biol.* **2006**, *10*, 11; c) T. Haruyama, *Adv. Drug Delivery Rev.* **2003**, *55*, 393.
[5] a) P. Alivisatos, *Nat. Biotechnol.* **2004**, *22*, 47; b) X. Gao, L. Yang, J. A. Petros, F. F. Marshall, J. W. Simons, S. Nie, *Curr. Opin. Biotechnol.* **2005**, *16*, 63; c) R. C. Somers, M. G. Bawendi, D. G. Nocera, *Chem. Soc. Rev.* **2007**, *36*, 579.
[6] Luminescent molecules were recently incorporated into zirconium phophate nanoparticles. See: M. Roming, H. Lünsdorf, K. E. J. Dittmar, C. Feldmann, *Angew. Chem.* **2010**, *122*, 642; *Angew. Chem. Int. Ed.* **2010**, *49*, 632.
[7] Phosphorescent dyes have been incorporated into silica matrices using electrostatic interactions, albeit at much lower loadings. See: a) X. He, H. Nie, K. Wang, W. Tan, X. Wu, P. Zhang, *Anal. Chem.* **2008**, *80*, 9597; b) W. Lian, S. A. Litherland, H. Badrane, W. Tan, D. Wu, H. V. Baker, P. A. Gulig, D. V. Lim, S. Jin, *Anal. Biochem.* **2004**, *334*, 135; c) X. Zhao, R. P. Bagwe, W. Tan, *Adv. Mater.* **2004**, *16*, 173; d) W. J. Rieter, J. S. Kim, K. M. L. Taylor, H. An, W. Lin, T. Tarrant, W. Lin, *Angew. Chem.* **2007**, *119*, 3754; *Angew. Chem. Int. Ed.* **2007**, *46*, 3680.
[8] R. Robson, *Dalton Trans.* **2008**, 5113.
[9] a) L. J. Murray, M. Dinca, J. R. Long, *Chem. Soc. Rev.* **2009**, *38*, 1294; b) L. Ma, D. J. Mihalcik, W. Lin, *J. Am. Chem. Soc.* **2009**, *131*, 4610; c) H. Furukawa, N. Ko, Y. B. Go, N. Aratani, S. B. Choi, E. Choi, A. O. Yazaydin, R. Q. Snurr, M. O'Keeffe, J. Kim, O. M. Yaghi, *Science* **2010**, *329*, 424; d) K. Uemura, S. Kitagawa, K. Fukui, K. Saito, *J. Am. Chem. Soc.* **2004**, *126*, 3817.
[10] O. R. Evans, W. Lin, *Acc. Chem. Res.* **2002**, *35*, 511.

[11] a) B. Chen, L. Wang, Y. Xiao, F. R. Fronczek, M. Xue, Y. Cui, G. Qian, *Angew. Chem.* **2009**, *121*, 508; *Angew. Chem. Int. Ed.* **2009**, *48*, 500; b) A. Lan, K. Li, H. Wu, D. H. Olson, T. J. Emge, W. Ki, M. Hong, J. Li, *Angew. Chem.* **2009**, *121*, 2370; *Angew. Chem. Int. Ed.* **2009**, *48*, 2334; c) Z. Xie, L. Ma, K. E. deKrafft, A. Jin, W. Lin, *J. Am. Chem. Soc.* **2009**, *132*, 922.

[12] a) L. Ma, C. Abney, W. Lin, *Chem. Soc. Rev.* **2009**, *38*, 1248; b) C.-D. Wu, A. Hu, L. Zhang, W. Lin, *J. Am. Chem. Soc.* **2005**, *127*, 8940; c) J. Lee, O. K. Farha, J. Roberts, K. A. Scheidt, S. T. Nguyen, J. T. Hupp, *Chem. Soc. Rev.* **2009**, *38*, 1450; d) F. Song, C. Wang, J. M. Falkowski, L. Ma, W. Lin, *J. Am. Chem. Soc.* **2010**, *132*, 15390; e) L. Ma, J. M. Falkowski, C. Abney, W. Lin, *Nat. Chem.* **2010**, *2*, 838.

[13] a) W. Lin, W. J. Rieter, K. M. L. Taylor, *Angew. Chem.* **2009**, *121*, 660; *Angew. Chem. Int. Ed.* **2009**, *48*, 650; b) J. Della Rocca, W. Lin, *Eur. J. Inorg. Chem.* **2010**, 3725; c) R. C. Huxford, J. Della Rocca, W. Lin, *Curr. Opin. Chem. Biol.* **2010**, *14*, 262; d) A. M. Spokoyny, D. Kim, A. Sumrein, C. A. Mirkin, *Chem. Soc. Rev.* **2009**, *38*, 1218.

[14] W. J. Rieter, K. M. L. Taylor, W. Lin, *J. Am. Chem. Soc.* **2007**, *129*, 9852.

[15] a) P. Horcajada, T. Chalati, C. Serre, B. Gillet, C. Sebrie, T. Baati, J. F. Eubank, D. Heurtaux, P. Clayette, C. Kreuz, J.-S. Chang, Y. K. Hwang, V. Marsaud, P.-N. Bories, L. Cynober, S. Gil, G. Ferey, P. Couvreur, R. Gref, *Nat. Mater.* **2010**, *9*, 172; b) W. J. Rieter, K. M. L. Taylor, H. An, W. Lin, W. Lin, *J. Am. Chem. Soc.* **2006**, *128*, 9024; c) K. M. L. Taylor, A. Jin, W. Lin, *Angew. Chem.* **2008**, *120*, 7836; *Angew. Chem. Int. Ed.* **2008**, *47*, 7722.

[16] K. E. deKrafft, Z. Xie, G. Cao, S. Tran, L. Ma, O. Z. Zhou, W. Lin, *Angew. Chem.* **2009**, *121*, 10085; *Angew. Chem. Int. Ed.* **2009**, *48*, 9901.

[17] W. J. Rieter, K. M. Pott, K. M. L. Taylor, W. Lin, *J. Am. Chem. Soc.* **2008**, *130*, 11584.

[18] Single-crystal X-ray diffractometer system equipped with a Cu target X-ray tube ($\lambda = 1.54178$ Å). Crystal data for LRuZn MOF: Triclinic, space group $P\bar{1}$, $a = 9.4196(2)$, $b = 14.0381(4)$, $c = 18.0896(4)$ Å, $\alpha = 83.244(2)$, $\beta = 75.876(2)$, $\gamma = 76.670(2)°$, $V = 2252.46(9)$ Å3, $\rho_{calcd} = 1.418\ g\,cm^{-3}$. CCDC 804313 contains the supplementary crystallographic data for this paper. These data can be obtained free of charge from The Cambridge Crystallographic Data Centre via www.ccdc.cam.ac.uk/data_request/cif.

[19] C. A. Kent, B. P. Mehl, L. Ma, J. M. Papanikolas, T. J. Meyer, W. Lin, *J. Am. Chem. Soc.* **2010**, *132*, 12767.

[20] a) Q. Fu, C. Lu, J. Liu, *Nano Lett.* **2002**, *2*, 329; b) Y. Lu, Y. Yin, B. T. Mayers, Y. Xia, *Nano Lett.* **2002**, *2*, 183.

[21] J. H. Cavka, S. Jakobsen, U. Olsbye, N. Guillou, C. Lamberti, S. Bordiga, K. P. Lillerud, *J. Am. Chem. Soc.* **2008**, *130*, 13850.

[22] B. J. Vilner, C. S. John, W. D. Bowen, *Cancer Res.* **1995**, *55*, 408.

[23] a) S. Li, Y. C. Chen, M. J. Hackett, L. Huang, *Mol. Ther.* **2008**, *16*, 163; b) C. S. John, B. J. Vilner, B. C. Geyer, T. Moody, W. D. Bowen, *Cancer Res.* **1999**, *59*, 4578; c) R. Banerjee, P. Tyagi, S. Li, L. Huang, *Int. J. Cancer* **2004**, *112*, 693.

